# Effect of mixing methods and chemical concentrations on the homogeneity of SiO$_2$ microsphere via Stöber and modified Stöber methods

Komkrit Petsong[a], Chumphon Luangchaisri[b], Chivarat Muangphat[a,*]

[a] Materials Technology program, School of Energy, Environment and Materials (SEEM), King Mongkut's University of Technology Thonburi, Bangkok 10140 Thailand

[b] Department of Physics, Faculty of Science, King Mongkut's University of Technology Thonburi, Bangkok 10140 Thailand

*Corresponding author, e-mail: chivarat.mua@kmutt.ac.th

**ABSTRACT**: Different mixing processes and chemical compositions were performed using the Stöber and modified Stöber methods to improve the homogeneity of SiO$_2$ microspheres. The direct mixing process with proper stirring speed (300 rpm) and duration (24 h) produced an excellent uniform size of 0.38 µm with a relative standard deviation (RSD) of 5.26% compared to the 0.38 µm with 18.41% RSD produced by the injection mixing process. In addition to the mixing process, the concentrations of tetraethyl orthosilicate (TEOS), H$_2$O, and NH$_3$ also affect the hydrolysis and condensation reaction rate. However, excessive concentrations of these chemicals can cause an imbalance in the reaction rates and aggregation process, leading to a multi-modal distribution. A mixture of 0.25 mol/l TEOS, 4.0 mol/l H$_2$O, and 1.0 mol/l NH$_3$ in ethanol produced highly uniform monodispersed SiO$_2$ particles of 0.48 µm size with a small deviation of 6.25% RSD. It was found that K cations can modify the structure of the Stern layer, increasing the particle size from 0.49 to 1.15 µm but widening its distribution from 6.12% to 21.74% RSD, due to the fast diffusion and aggregation of the oligomer or primary particles. The bi-directional mixing method can increase the uniformity of SiO$_2$ microspheres, reducing their RSD to 6.6% by creating a strong turbulence force through 30 cycles per hour of reversed mixing. This study demonstrates that the Stöber and modified Stöber methods can synthesize high-circularity SiO$_2$ particles (between 0.93 and 0.97) with an improved particle size distribution.

**KEYWORDS**: Stöber method, modified Stöber method, silicon dioxide, bi-directional mixing

## INTRODUCTION

Nanoparticles have attracted significant attention because of their superior and unique properties that distinguish them apart from their bulk materials and enable them to be applied in numerous fields [1]. In particular, complex-structure nanoparticles like hollow, core/shell, and multilayer [2, 3] have exhibited great potential in various applications. The use of complex-structure nanoparticles has increased exponentially over simple spherical particles due to their higher surface area, physico- and electrochemical properties, and functionalizability [4–6].

Silicon dioxide (SiO$_2$) is an interesting sacrificial core material for creating hollow, core/shell, or multilayer structures in spherical nanoparticles because it is easy to synthesize, tolerates high temperatures, has high catalytic activity, is chemically inert, and can be adjusted in size [7–9]. The Stöber method is the most well-known, simple, reliable, controllable, and high-throughput process for synthesizing dispersed spherical SiO$_2$ particles discovered in 1968 by Wolfgang Stöber and colleagues [10]. The Stöber SiO$_2$ particles were synthesized by chemically reacting precursors with catalysts like water and ammonia [11, 12]. For over fifty years, researchers have systematically investigated reaction parameters such as precursor and cata-

lyst concentrations [13], types of alcohol [14, 15], and temperature [16] to produce monodispersed and uniform silica spheres. The production of SiO$_2$ particles with well-controlled physical and chemical properties provided the significant impact of these parameters on science and technology. Interest in the Stöber method has continued for a more comprehensive understanding of material properties and applications such as catalysis, carbon dioxide absorption, and drug delivery.

However, the original size of Stöber SiO$_2$ particles is limited to below 0.5 µm [17] due to the accumulation of negative charge at the Stern layer. To overcome this size limitation, the modified Stöber method was introduced, which delayed the formation of the electric double layer (EDL) of the SiO$_2$ surface using an adsorption cationic surfactant technique [18–20].

The growth mechanism of the SiO$_2$ particle can be continued by depositing cations on the particle surface, to reduce the suspension intermediate state and to allow the cations to adhere to the SiO$_2$ surface. Studies indicate that the effectiveness of reducing the surface potential of inorganic salts, such as NaCl, KCl, and LiCl, depends on their ionic radius [21, 22]. Despite significant efforts that have been devoted to control the size and monodispersity of SiO$_2$ particles by adding catalysts to increase the diffusion of intermediate substances, the homogeneous deposition of intermediates

remains challenging, leading to a broad size distribution. A spherical and uniformly sized sacrificial core material can improve the efficacy of nanoparticles with desired or preferable properties.

This report examines how the concentration of TEOS and catalyst affects the synthesis kinetics (hydrolysis and condensation reactions), nuclei formation, and particle growth, which Stöber and colleagues also investigated. It also investigates certain factors that received low prioritized attention due to their minimal impact on particle formation but can improve the roundness and size distribution of $SiO_2$ particles. These factors include the mixing process (direct and injection) and mixing parameters (stirring speed and duration). All experiments were conducted at room temperature for 24 h using a magnetic stirrer.

## Modified Stöber method

As mentioned previously, the negative potential of the $SiO_2$ surface prevents the deposition of silanol monomers and oligomers on the particle surfaces, which limits the growth mechanism and ultimately impacts the size of the particles. Due to the large size of potassium cation, different concentrations of KCl (1.0, 2.0, 3.0, 4.0, and 5.0 mmol/l) were added to the catalyst reagents (4.0 mol/l $H_2O$ and 1.0 mol/l $NH_3$ in ethanol) before mixing with TEOS precursor (0.25 mol/l in ethanol). The effects of operating temperature (0, 25, and 50 °C) and bi-directional stirring cycles (0, 10, 20, and 30 cycles) were studied individually to develop particle uniformity and circularity, as illustrated in Fig. 1(c).

## Characterizations

The surface morphologies of monodispersed $SiO_2$ particles were observed using field emission scanning electron microscopy (FE-SEM) with a secondary electron detector (SED) mode. The FE-SEM instrument used for this purpose was the Phenom Pharos G2 model, manufactured by Thermo Fisher Scientific (Oregon, USA), which operated at 10 kV. The high-resolution SEM micrographs were utilized to analyze the average size, size distribution, and circularity of the $SiO_2$ particles using the "Analyze Particles" function in ImageJ, and the effectiveness of the bi-directional stirring in improving microsphere homogeneity.

## MATERIALS AND METHODS

### Materials

Tetraethyl orthosilicate (TEOS) (⩾99%) was purchased from Sigma Aldrich (Missouri, USA). Ethanol absolute (⩾99.9%, AR grade) was purchased from Merck (Darmstadt, Germany). Ammonium solution (28% $NH_3$ dissolved in water, AR Grade) was purchased from QRëC™ (Auckland, New Zealand). Potassium chloride (extra pure KCl, AR Grade) was purchased from AJAX-Finechem (New South Wales, Aus-

tralia). Deionized (DI) water was used in all experiments.

## Stöber methods

### Synthesis of $SiO_2$ via direct mixing method

The TEOS precursor (0.3 mol/l in ethanol) was directly mixed with the catalyst reagent (a mixture of 4.0 mol/l $H_2O$ and 1.0 mol/l $NH_3$ in ethanol) using a magnetic stirrer. The experiments were conducted at room temperature with different vigorous stirring speeds (0, 150, 300, and 600 rpm.) for 24 h, as illustrated in Fig. 1(a). A volume of 1 ml of the colloidal solution was collected after mixing for 1, 3, 6, 9, 12, and 24 h and cleaned with ethanol.

### Synthesis of $SiO_2$ via injection mixing method

In the injection mixing process, $SiO_2$ particles were prepared by dripping the TEOS precursor (0.3 mol/l in ethanol) into the catalyst agent (a mixture of 4.0 mol/l $H_2O$ and 1.0 mol/l $NH_3$ in ethanol) at a rate of 0.1 ml/min controlled by a syringe pump (Fig. 1(b)). The drop of TEOS precursor was suspended in the catalyst agent using a magnetic stirrer with a stirring speed of 300 rpm at room temperature. After mixing, the particles were collected and sampled under the same conditions as the direct mixing.

### Synthesis of $SiO_2$ with different chemical concentrations

The Stöber method utilizes $NH_3$, TEOS, and $H_2O$ as the primary catalyst agents for synthesizing the $SiO_2$ particles. It was necessary to conduct individual investigations to understand how the concentration of chemicals influences the size distribution and circularity of monodispersed $SiO_2$ particles. To achieve this study, the $NH_3$ concentrations were varied (0.5, 1.0, 2.0, 3.0, 4.0, and 5.0 mol/l) in a mixture of 4.0 mol/l $H_2O$ in ethanol. These catalyst reagents were directly mixed with the TEOS precursor (0.1 mol/l in ethanol) using a magnetic stirrer. After that, an ethanolic mixture of 4.0 mol/l $H_2O$ and 1.0 mol/l $NH_3$ was prepared and then combined with different TEOS concentrations (0.1, 0.2, 0.25, 0.3, 0.4, 0.5, as proposed by Mazzoli and Favoni [23], which was utilized to determine the diameter and circularity of 300 to 600 particles in each condition.

The image dimensions in pixel are correlated to physical dimensions with the scale bar. The length of the scale bar was set as a known distance in μm for calculating the particle diameter. The gray-level SEM micrograph was converted from RGB color to 8-bit gray scale through proper thresholding. Then, the lower and upper threshold values were automatically set to separate the signal from the background. An accurate size measurement is automatically running
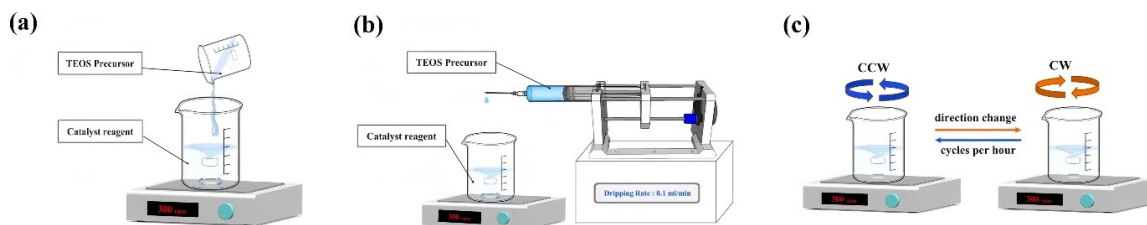
**Fig. 1** Illustration of the experimental setup of (a) direct and (b) injection mixing processes on the synthesized $SiO_2$ particles via a Stöber method. (c) The bi-directional mixing method on the synthesized $SiO_2$ particles via a modified Stöber method.

by the image analysis system "Analyze particles". Additionally, "Analyze particles" also can describe the circularity of spherical particle using the diameter in every dimension, which should be a single number due to an equivalent spherical diameter.

After that, the average particle size, standard deviation, and relative standard deviation were calculated following the Eqs. (1), (2), and (3), respectively.

$$\text{Average particle size:} \quad \mu = \frac{1}{n}\sum_{i}^{n} x_i \tag{1}$$

$$\text{Standard deviation:} \quad \sigma = \sqrt{\frac{1}{n}\sum_{i}^{n}(x_i - \mu)^2} \tag{2}$$

Relative standard deviation (RSD):

$$\text{RSD} = \left(\frac{\sigma}{\mu}\right) \times 100 \tag{3}$$

where $n$ is the total number of values, $x_i$ represents each individual value in the dataset.
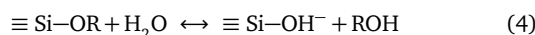
In addition, the amorphous phase of $SiO_2$ particles was detected using a D8 Advance X-ray diffractometer (Bruker, Karlsruhe, Germany) with Cu-Ka radiation ($\lambda$ = 1.540 Å) and $2\theta$ ranging from 20° to 80°, while the surface charge of the $SiO_2$ particles was quantified by a zeta potential analyzer (Zetasizer nano) manufactured by Malvern Panalytical (Worcestershire, England).
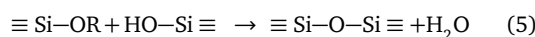
**RESULTS AND DISCUSSION**

A series of experiments were conducted to investigate the influence of the synthesis parameters and chemical concentration on the nucleation and growth mechanism of $SiO_2$ particles via the Stöber and modified Stöber methods. These experiments aimed to create monodisperse $SiO_2$ particles with a perfect spherical shape and narrow size distribution. The $SiO_2$ particles were synthesized through the Stöber method, which begins with the hydrolysis of tetraethyl orthosilicate $(Si(OC_2H_5)_4$; TEOS) and $H_2O$ to produce the silanol monomers $(Si(OH_{(4-x)})_x)$, as shown in Eq. (4). These hydrolyzed silanol monomers then undergo water/alcohol condensation reactions to form oligomers, according to Eqs. (5) and (6) [24].
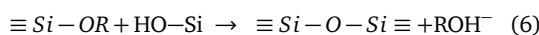
Hydrolysis reaction

$$\equiv Si{-}OR + H_2O \;\longleftrightarrow\; \equiv Si{-}OH^- + ROH \tag{4}$$

Water condensation

$$\equiv Si{-}OR + HO{-}Si \equiv \;\rightarrow\; \equiv Si{-}O{-}Si \equiv + H_2O \tag{5}$$

Alcohol condensation

$$\equiv Si{-}OR + HO{-}Si \;\rightarrow\; \equiv Si{-}O{-}Si \equiv + ROH^- \tag{6}$$

Upon reaching the supersaturation point, oligomers immediately aggregate and polymerize with each other via diffusional transport to form $SiO_2$ nuclei and grow to final size by aggregating with the residual intermediate [20]. The growth mechanism of $SiO_2$ particles discontinues when the oligomer accumulation reaches a point where they create a strong negative electrostatic potential that repels the diffusion of silanol monomers. To overcome this, the modified Stöber method was employed to alter the particle's charge by manipulating its electrostatic potential.

Different concentrations of KCl were added during the growth process to supply cations and increase the size of $SiO_2$ particles when the operating temperature influence the chemical reaction rate and growth mechanism. Furthermore, a bi-directional mixing process was recruited to improve the homogeneous growth of $SiO_2$ microspheres, leading to a narrow size distribution.

**The influence of mixing parameters**

**Holding time**

Hydrolysis and condensation reactions occur rapidly, when compared to the diffusion and aggregation of the residual intermediates, which require more time to produce $SiO_2$ particles of the final size. The synthesis experiments were performed by directly mixing the precursor solution and catalytic agents under vigorous stirring to determine the appropriate reaction time and understand how holding time affects the size, size distribution, and circularity of the synthesized particles.

The data presented in Fig. 2 indicates that the average size of the synthesized particles increased from
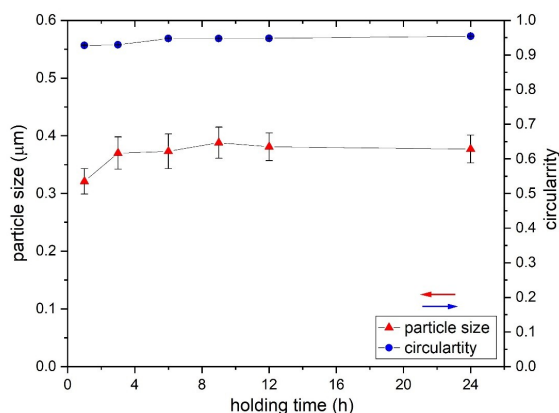
**Fig. 2** The effect of holding time on the size and circularity of SiO$_2$ particles.

0.32 to 0.38 µm as the holding time increased from 1 to 3 h. The error bars in the graph indicate the standard deviation of SiO$_2$ particles, calculated with ImageJ using at least 400 particles. After a holding time of 3 h, the average particle size remained stable because the reagent concentration was too low to continue the growth mechanism. These results are consistent with Stöber's study in 1968, which suggested that the total reaction time should be approximately 120 min [10]. After 3 h, the relative standard deviation of SiO$_2$ particles slightly decreased from 6.25% to 5.26% as the circularity of SiO$_2$ particles slightly improved from 0.93 to 0.95. Additionally, the particle size and size distribution remained consistent after 24 h. Based on these results, further experiments were conducted for 24 h to ensure the complete synthesis of uniform monodisperse SiO$_2$ particles.

**Stirring speed**

Fig. 3(a) shows that the stirring speed did not affect the average size of the particles, which was approximately 0.38 µm. The SEM image of the SiO$_2$ particles synthesized through the direct mixing without agitation shows multiple gel networks between particles, produced by residual silanol monomers (red circles). The lack of agitation produces a broad relative size distribution (10.53% RSD) due to the non-homogeneous distribution of TEOS in the system. Increasing the stirring speed from 150 to 300 rpm improves the homogeneity of the solution, reduces the relative standard deviation of SiO$_2$ particles from 7.89% to 5.26%, and helps to eliminate the residue gel networks.

At a stirring speed of 600 rpm, a strong convection force slightly reduced the size of synthesized SiO$_2$ particles from 0.38 to 0.32 µm because it interrupted the deposition of oligomers. The increased stirring speed also expanded the relative standard deviation

of SiO$_2$ particles from 5.26% to 7.89%. Additionally, it slightly improved the particle circularity from 0.93 to 0.95, which is caused by the collisions between particles in strong convection force. According to Fernandes et al [25], faster-stirring speed increases the number of collisions among particles and promotes their coagulations, leading to a multi modal distribution.

However, a solid conventional force, generated at a stirring speed of 600 rpm, interrupted the deposition of oligomers, resulting in a decrease in the size of synthesized SiO$_2$ particles from 0.38 to 0.32 µm, accompanied by a slight improvement in the particle circularity from 0.93 to 0.95.

Based on these results, the stirring speed plays a significant role in producing a uniform solution and achieving a narrow size distribution of SiO$_2$. After observing the significant changes in both the particle size and size distribution, a stirring speed of 300 rpm was selected for subsequent experiments, since it has the potential to produce larger particles with a narrow standard deviation.

**Mixing process**

All experiments comparing the different mixing processes were done by combining two ethanolic solutions with a precursor (0.1 mol/l TEOS) into another catalytic agent (1.0 mol/l NH$_3$ with 4.0 mol/l H$_2$O). Fig. 4(c) shows that the monodisperse SiO$_2$ particles synthesized through direct and injection mixing methods have the same equivalent diameter, approximately 0.38 µm, even though their relative standard deviations are distinct, 5.26% and 21.05%, respectively.

The injection mixing process results in a broad distribution of SiO$_2$ particle sizes, likely due to variations in chemical concentrations and growth periods at different dripping times. On the other hand, the direct mixing process offers more circular particles compared to those obtained from injection mixing, with circularity values of approximately 0.97 and 0.95, respectively. These results suggest that the direct mixing method produces silanol monomers through a hydrolysis reaction, allowing them to homogeneously condense on the particle surface, forming spherical particles. The surface charge of SiO$_2$ particles controls the equivalent deposition of silanol monomers, oligomers, or other particles during the growth period of SiO$_2$ particles.

Chang et al [26] mentioned that the SiO$_2$ particles exhibited monotonic growth when the concentration of silanol monomers reached above the saturated level. Furthermore, adding more TEOS led to an increase in the concentration of silanol monomers exceeding the critical level, forming secondary particles. This condition led to the observation of multi modal particles, which were attributed to the formation of secondary particles and those that developed from primary parti-
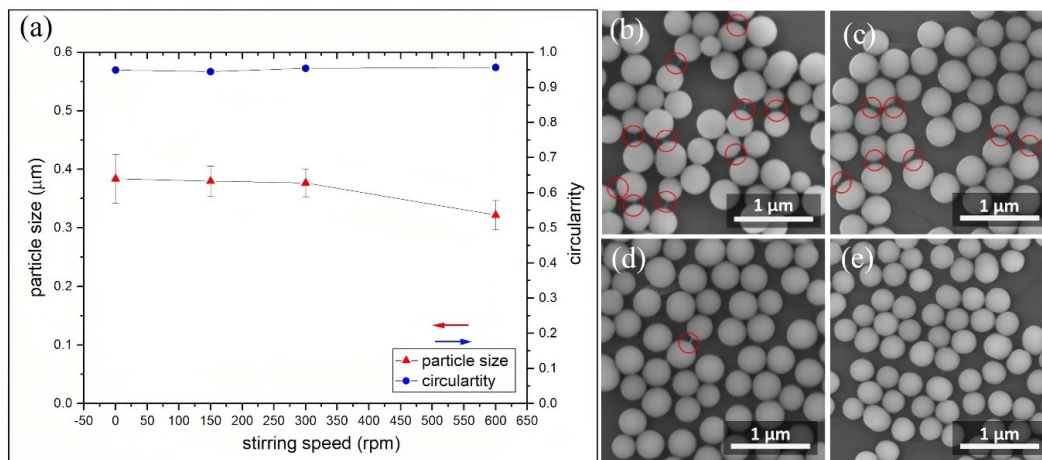
**Fig. 3** (a) The influence of stirring speed on the particle size and circularity of $SiO_2$ particles. (b–e) FE-SEM images showing how varying the stirring speed (0, 150, 300, and 600 rpm, respectively) eliminates the linkage from the gelation (red circles) obtained during the sol-gel (Stöber) method.
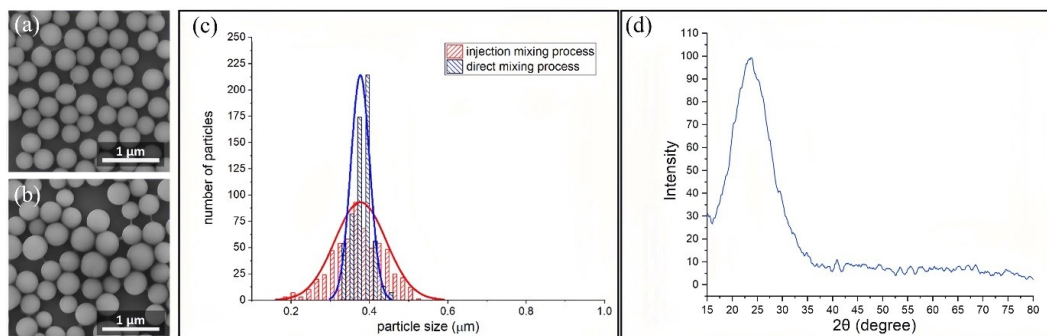


**Fig. 4** SEM images of synthesized $SiO_2$ particles from (a) direct and (b) injection mixing processes. (c) The size distribution examined by ImageJ software, and (d) X-ray diffraction pattern of amorphous structure of $SiO_2$ particles.

cles.

Additionally, the diffraction pattern of the $SiO_2$ particles synthesized via the direct mixing process shows a peak centered around 22°, corresponding to the amorphous structure of synthesized $SiO_2$ particles (JCPDS 29-0085), as depicted in Fig. 4(d). The direct mixing process was preferred for conducting further experiments in order to study the influence of other parameters on the size, shape, and uniformity of monodisperse $SiO_2$ particles.
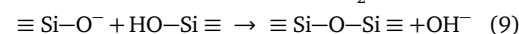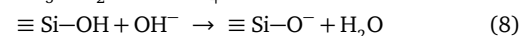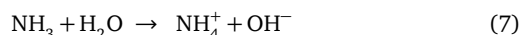
**The effect of chemical concentration**

**Ammonia concentration**

The impact of $NH_3$ was assessed by adding it in different amounts into an ethanolic solution (4.0 mol/l $H_2O$ in ethanol), producing $NH_3$ concentrations ranging from 0.5 to 5.0 mol/l. This mixture was then added and suspended in an ethanolic solution of precursor (0.3 mol/l TEOS) using a direct mixing process at 300 rpm stirring speed for 24 h. As shown

in Fig. 5(a), increasing the $NH_3$ concentration from 0.5 to 1.0 mol/l developed larger particles with a size of 0.16 to 0.39 µm.

$NH_3$ molecules were partially decomposed into ammonium ions ($NH_4^+$) through the dissociation of $H_2O$ molecules. This rapid ionization produced nucleophilic hydroxyl anions (OH-) within the solution. Then, the ionized hydroxyl anion reacted with the silicon atom on the TEOS molecule to form the silanol monomers, as illustrated in Eqs. (7), (8), and (9) [19].

Ammonia ionization

$$NH_3 + H_2O \rightarrow NH_4^+ + OH^- \tag{7}$$

$$\equiv Si-OH + OH^- \rightarrow \equiv Si-O^- + H_2O \tag{8}$$

$$\equiv Si-O^- + HO-Si \equiv \rightarrow \equiv Si-O-Si \equiv + OH^- \tag{9}$$

The concentration of $NH_3$ affects the formation of hydroxyl anions and the number of oligomers through the hydrolysis reaction.

The nucleation period was prolonged at 0.5 mol/l $NH_3$ concentration because of the low hydrolysis reac-
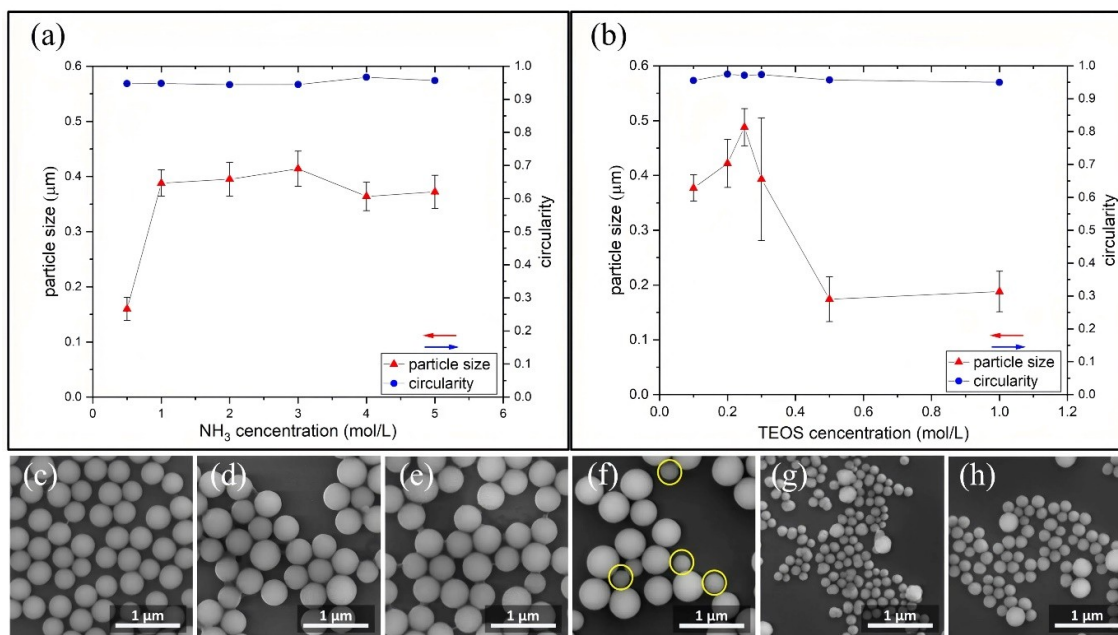
**Fig. 5** The effect of (a) $NH_3$ and (b) TEOS concentrations on the particle size and circularity of $SiO_2$. (c–h) SEM images of synthesized $SiO_2$ particles from 0.1, 0.2, 0.25, 0.3, 0.5, and 1.0 mol/l TEOS concentration, respectively.

tion rate. Partially hydrolyzed silanol monomers were formed, continuously grew, and reached a certain size, while the remaining TEOS precursors began to hydrolyze. This condition led to the production of small average-sized particles (0.16 μm) and broadly distributed $SiO_2$ particles (18.00% RSD), consistent with the findings of Yandong et al [20], Kangtaek et al [27], and Dongming et al [28].

When the $NH_3$ concentration exceeded 1.0 mol/l, the mean size of $SiO_2$ particles dramatically increased from 0.16 to 0.39 μm, resulting in the formation of more hydrolyzed silanol monomers. This analogous growth stage produced a narrow size distribution (5.13% RSD) of $SiO_2$ particles, as reported in the study from Yang et al [20].

Beyond this point, the mean size of $SiO_2$ particles slightly stabilized, ranging from 0.36 to 0.41 μm due to the limitation of the TEOS concentration. Besides, the difference in size distribution (between 7.32% and 8.33% RSD) and circularity (between 0.94 and 0.97) were hardly noticeable. Van and Kentgens [29] also proposed that the high concentration of $NH_3$ (>1.0 mol/l) increased the ionic strength and led to a decrease in colloidal stability due to the high concentration of $NH_4^+$ and $OH^-$ ions. This situation would result in a decrease in the double-layer thickness, causing the $SiO_2$ particles to aggregate. However, the particles in this report remained well-dispersed even when the concentration of $NH_3$ reached 5.0 M [30].

These results indicate that ammonium ions worked as a primary catalyst, accelerating the conden-

sation reaction, controlling the formation mechanism of silanol monomers during the nucleation stage, and facilitating the aggregation of $SiO_2$ particles. In the subsequent experiment, 1.0 mol/l $NH_3$ was preferred to reduce chemical usage and pose fewer risks to researchers.

**TEOS concentration**

Fig. 5(b) shows the effects of TEOS concentration (0.1 to 1.0 mol/l in ethanol) on the size and circularity of $SiO_2$ particles, which were produced by directly mixing for 24 h the precursor solution (TEOS in ethanol) with the catalyst solution (4.0 mol/l $H_2O$ and 1.0 mol/l $NH_3$ in ethanol). The average size of the $SiO_2$ particles gradually increased (0.38 to 0.49 μm) as the TEOS concentration increased (0.1 to 0.25 mol/l), likely due to the increased availability of the silanol monomers. Increasing the TEOS concentration accelerates the hydrolysis reaction rate, producing more silanol monomers, ultimately resulting in larger $SiO_2$ particle sizes. However, the SEM image shows a multimodal distribution of particles when the TEOS concentration becomes too high (0.3 mol/l), as highlighted by the yellow circles in Fig. 5(f).

The multi modal distribution occurs when the concentration of redundant oligomers increases rapidly, reaching the saturation point and suddenly aggregating to form the primary particle. However, when irrelevant oligomers and monomers reach their critical volumes, which depend on their surface charge, they can-
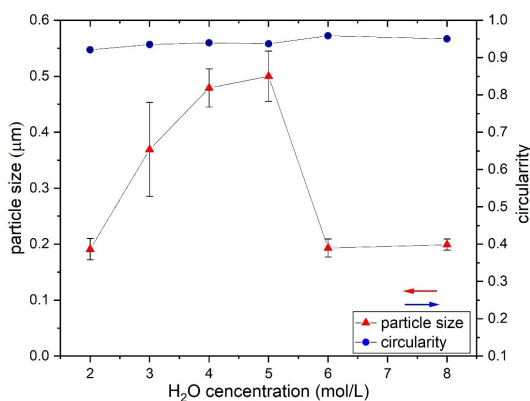
**Fig. 6** The influence of $H_2O$ concentrations in ethanol on the particle size and circularity of $SiO_2$.

not aggregate with the primary particle, leading to the formation of secondary particles. The presence of secondary particles (multi modal distribution) reduces the mean size of $SiO_2$ particles (0.39 µm) while showing an extensive distribution (28.21% RSD). Similar conclusions regarding the formation of large-size and high-polydisperse particles produced at high concentrations of TEOS were also reached by Bogush et al [11] and Harris et al [31].

Beyond a certain point, massive nuclei are rapidly generated due to excessive aggregation of oligomers caused by a very short inter-distance. The results showed that the average final size of particles decreased to 0.17 µm and stabilized at 0.19 µm, due to an inadequate ammonia concentration to promote the condensation reaction, as indicated in Fig. 5(g,h). Rao et al [32] also identified this behavior and stated that particle size decreased with increasing TEOS concentration, resulted in smaller particles.

The amount of TEOS had a noticeable effect on the particle size and distribution of $SiO_2$ but had an insignificant influence on their circularity, which remained between 0.95 and 0.97. The concentration of TEOS affected the nucleation and growth rates by influencing the supersaturation level of silanol monomers. Therefore, 0.25 mol/l TEOS was found to be an optimal concentration for synthesizing $SiO_2$ particles with high circularity (0.97), large size (0.49 µm), and narrow relative standard deviation (6.12%), which aligns with Stöber's result [10]. This concentration was chosen for synthesizing $SiO_2$ particles in the subsequent investigation.

**Water concentration**

Fig. 6 demonstrates how the concentration of $H_2O$ affects the particle size, distribution, and circularity of $SiO_2$ when the $H_2O$ concentration in ethanol increases from 2.0 to 8.0 mol/l. The average particle size increases from 0.19 to 0.50 µm, due to the accelerating hydrolysis reaction rate caused by the increase in $H_2O$ concentration from 2.0 to 5.0 mol/l. However, when the $H_2O$ concentration increases further, the size of $SiO_2$ particles decreases significantly from approximately 0.50 to 0.21 µm, due to the increasing in the separation distance between monomers.

The findings confirm that the concentration of $H_2O$ plays a crucial role in nucleation by regulating the speed of the hydrolysis reaction, the formation of nuclei, and the rate of growth. Van Helden et al [33] also reached a similar conclusion. They also investigated the bell-shaped curve representing the effect of $H_2O$ concentration. The particle size increased with increasing $H_2O$ concentration and then decreased when the concentrations went beyond the optimum point. This result is consistent with the results of Stöber et al [10] and Bogush et al [11].

Although the particles synthesized from 2.0, 6.0, and 8.0 mol/l $H_2O$ in ethanol have practically identical diameters (between 0.19 and 0.20 µm), higher $H_2O$ concentration provides better circularity (0.96) than the case of lower concentration (0.92). Furthermore, lower $H_2O$ concentration (2.0 mol/l) generates insufficient active silanol monomers, which impacts the ability to balance the surface charge by deposition, thereby impacting the shape of $SiO_2$ particles. Giesche [34] also verified this evidence by considering the influence of the particle size on its shape. At higher $H_2O$ concentrations, the particles become perfectly smooth spheres.

For the subsequent experiment, a $H_2O$ concentration of 4.0 mol/l was selected, providing particles with larger size, narrower size distribution, and excellent circularity. After evaluating the effects of chemical concentration parameters, the results show that the ratio of TEOS to $H_2O$ is crucial to controlling the homogeneous size of $SiO_2$ particles by balancing the nucleation and aggregation process. In contrast, the additional $NH_3$ does not affect the size distribution of the particles but rather only increases their overall size.

**The effect of parameters via the modified Stöber method**

**Potassium chloride concentration**

The graph in Fig. 7 shows the size and distribution of spherical $SiO_2$ particles synthesized under different concentrations of KCl, ranging from 0 to 4 mmol/l. Notably, in the absence of KCl, the average and distribution of particle sizes are remarkable, measuring 0.49 µm and 6.12% RSD, respectively. The growth of $SiO_2$ particles stops once they reach approximately 0.5 µm in size. This is due to the formation of a strong electric double layer, composed of Stern and diffusion layers, which prevents silanol monomers passing through the diffusion layer.
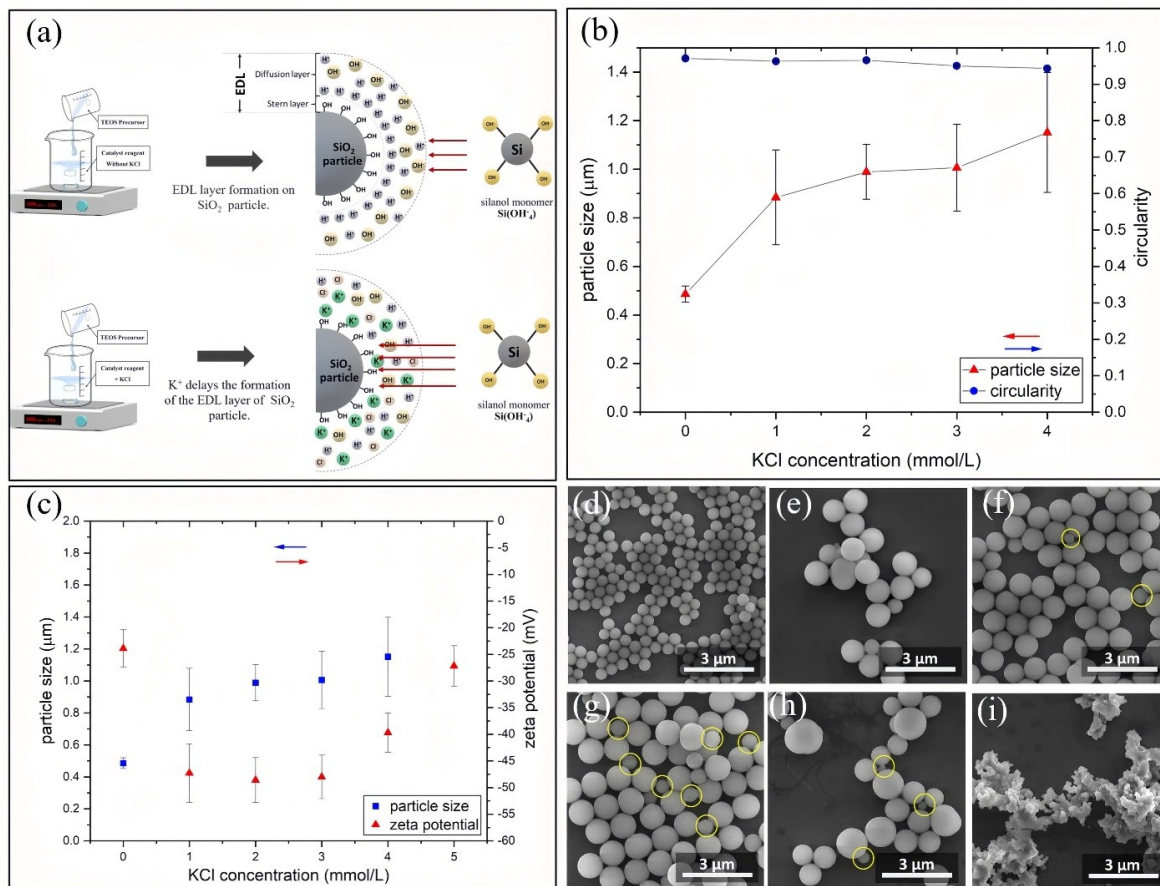
**Fig. 7** (a) Electric double layer (EDL) moderated by adding $K^+$ cations, (b) the influence of KCl on the size, circularity and (c) zeta potential of $SiO_2$ particles. SEM images of $SiO_2$ particles (d) without KCl, and (e–i) with different KCl concentrations of 1.0, 2.0, 3.0, 4.0, and 5.0 mM in ethanol, respectively.

This repulsive force of the electric double layer can be reduced by adding positive ions of inorganic salts, as shown in Fig. 7(a), which allows the hydrolyzed silanol monomers to diffuse more easily and condense on the $SiO_2$ surface by associating with the Stern layer. The graph shows that the presence of potassium ions ($K^+$), at a concentration of 1 mmol/l in ethanol, has an extensive attraction effect, increasing the average size of $SiO_2$ particles up to 0.88 μm. Then, the average size of $SiO_2$ particles slightly reaches 1.15 μm when the concentration of KCl is increased to 4.0 mmol/l. At the same time, the addition of KCl also improves the distribution of particle size from 6.12% to 21.74% RSD, while slightly decreasing the particle circularity from 0.97 to 0.95. These results indicate that the facilitating $K^+$ ions enable continuous particle growth. Some previous studies also revealed that the addition of $K^+$ ions slightly decrease the electric surface potential while increasing the size of silica particles [35].

However, the uniformity of the intermediate deposition during the growth process can be difficult to control, due to the influence of the reduction agent. Specifically, the rapid deposition rate of intermediate suspension onto the unstable primary particles leads to a less spherical shape with multi-modal distribution, as depicted with yellow circles in Fig. 7(f–h). Furthermore, an experiment with a high concentration of KCl at 5.0 mmol/l agrees with Nakabayashi et al [21], which suggests that the overabundant positive charge of $K^+$ instantly accelerates the aggregation of small primary particles. This, in turn, changes the spherical shape of the final particles to an irregular form, as shown in the SEM image in Fig. 7(i).

The surface potential value does not directly relate to the concentration of KCl or the participation of $K^+$ at the particle surface but rather to the particle size itself. As shown in Fig. 7, particles of 0.49 μm size exhibit a zeta potential of $-23.9$ mV $\pm$ 3.5 mV. However, this becomes more negative ($-48.0$ mV $\pm$ 4.1 mV) when the particle size increases to 1.01 μm. Furthermore, the presence of smaller particles dramatically reduces the overall negative charge of the $SiO_2$ surface from
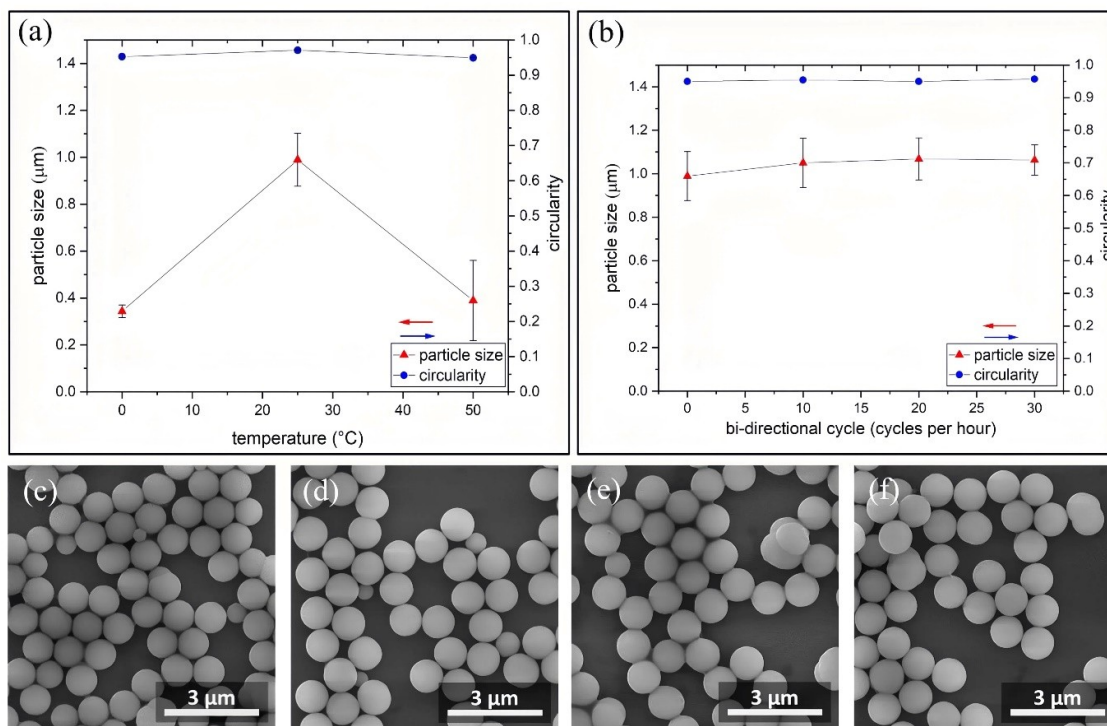
**Fig. 8** (a) The relationship between the operating temperature and the size and circularity of synthesized SiO$_2$ particles, (b) the improvement in size and circularity of synthesized SiO$_2$ particles using bi-directional stirring, and (c–f) SEM images of SiO$_2$ particles at different bi-directional cycles (0, 10, 20, and 30 cycles per hours).

−39.7 mV ± 3.7 to −27.2 mV ± 3.8 mV, as shown in Fig. 7(g,h). Based on these results, a KCl concentration of 2.0 mmol/l was chosen for the following experiments, as it provides a narrow size distribution (11.11% RSD) with good circularity (0.97).

**Temperature**

Fig. 8(a) illustrates the effect of temperature on the chemical reaction rate and final size of SiO$_2$ particles. These experiments were conducted using a modified Stöber method with a catalytic solution containing 2.0 mmol/l KCl and a temperature range of 0 to 50 °C over a period of 24 h. The result shows that, at 25 °C, the size of SiO$_2$ particles was approximately 0.99 µm, three times larger than the average particle size of SiO$_2$ (0.34 µm) at 0 °C after 24 h. However, the distribution also increased considerably from 8.82% to 11.11% RSD. In contrast, the circularity results show only minor variations (0.95–0.97).

The first experiment was conducted at 0 °C for 24 h. It was found that the average size of SiO$_2$ particles was approximately 0.34 µm due to the low hydrolysis and condensation reaction rate at low temperatures. The average size of SiO$_2$ particles increased to approximately 0.99 µm after 24 h when the operating temperature was around 25 °C, almost three

times larger than the average particle size of SiO$_2$ (0.39 µm) at 0 °C. However, the size distribution of 0 °C and 25 °C slightly increased from 8.82% to 11.11% RSD, but the size distribution dramatically increased when the temperature was raised to 50 °C (43.58% RSD). In contrast, the circularity results show only minor variations, ranging between 0.95 and 0.97.

Scientists also discovered that low temperatures result in a slow hydrolysis reaction rate, expanding the nucleation period. This process generates a small number of small particles, which can subsequently grow over an extended period. Most TEOS precursors undergo rapid hydrolysis at high temperatures, generating silanol monomers. The high hydrolysis reaction rate causes the concentration of silicic acid monomers to instantly reach the critical saturation level and generate SiO$_2$ nuclei through the condensation reaction [16, 36]. According to Tan et al [16] and Matsoukas et al [12], the hydrolysis reaction rate increases significantly compared to the rate of condensation reaction as temperature rises, leading to a decrease in the average size of the particles.

Additionally, Glesch [34] and Park et al [37] also verified that an increase in temperature raised the nucleation rate and shortened the nucleation period. Therefore, higher temperatures could produce more nuclei in a short inter-distance, providing smaller par-

ticles with narrower size distribution.

This suggests that the operating temperature controls the rate of the chemical reaction, which has an entirely different effect on the particle size and distribution. In conclusion, a temperature of 25 °C was selected for further investigation since it is the most suitable operating temperature for producing $SiO_2$ microspheres with high uniformity and circularity.

**Bi-directional mixing**

In the conventional mixing method, a magnetic bar and stirrer are commonly used to homogenize mixable liquids or disperse solid particles in liquids, with a specific flow pattern by rotating the magnetic stirrer in one direction. However, during the synthesis of $SiO_2$ particles, the particles tend to aggregate together at the container walls due to their weight and centrifugal force, resulting in a large size distribution of particles.

To address this issue, bi-directional stirring was used to increase the homogeneity of the solution by rotating the magnetic stirrer in opposite directions, creating a more turbulent flow pattern [20]. Experiments were conducted to compare the efficacy of one- and bi-directional stirring at different cycles (10, 20, and 30 cycles per hour). All experiments were conducted at the same stirring speed (300 rpm) and temperature (25 °C) for 24 h.

SEM images show the morphology of $SiO_2$ microspheres synthesized through one-directional (Fig. 8(c)) and bi-directional mixing processes at 10, 20, and 30 cycles per hour, respectively (Fig. 8(d–f)). As shown in Fig. 8(b), the average particle size only slightly changed from 0.99 to 1.06 μm, while the distribution significantly improved from 11.11% to 6.60% RSD with perfect circularity (0.96), when bi-directional cycles were increased to 30 cycles per hour. However, the 30 cycles per hour of bi-directional stirring was a limitation of this study because the fast and strong convection force may cause the solution to splash and a short period of reverse flow of the solution may not be enough to fully homogenize it.

**CONCLUSION**

The direct mixing process in the Stöber method results in a narrower size distribution and better circularity of $SiO_2$ particles than the injection mixing process due to the equivalent nucleation and growth period. The optimal concentration of precursor, catalyst, and reducing agent effectively controls the balance between nucleation and aggregation, producing particles with a homogeneous size and shape. In the modified Stöber method, potassium cations ($K^+$) reducing capability leads to excessive aggregation of intermediate substances, producing micron-sized $SiO_2$ particles with a wider size distribution. The homogeneity of the $SiO_2$ microspheres in the modified Stöber method can be improved by applying a proper turbulence force using the bi-directional stirring technique. It is important to note that the particle circularity strongly correlates with the narrow size distribution of $SiO_2$ particles.

**REFERENCES**

1. Khalid K, Tan X, Mohd Zaid HF, Tao Y, Lye Chew C, Chu D-T, Lam MK, Ho Y-C, et al (2020) Advanced in developmental organic and inorganic nanomaterial: a review. *Bioengineered* **11**, 328–355.
2. Joseph CG, Taufiq-Yap YH, Musta B, Sarjadi MS, Elilarasi L (2021) Application of plasmonic metal nanoparticles in $TiO_2$-$SiO_2$ composite as an efficient solar-activated photocatalyst: A review paper. *Front Chem* **8**, 568063.
3. Srdić VV, Mojić B, Nikolić M, Ognjanović S (2013) Recent progress on synthesis of ceramics core/shell nanostructures. *Process Appl Ceram* **7**, 45–62.
4. Li M, Cheng F, Xue C, Wang H, Chen C, Du Q, Ge D, Sun B (2019) Surface modification of Stöber silica nanoparticles with controlled moiety densities determines their cytotoxicity profiles in macrophages. *Langmuir* **35**, 14688–14695.
5. Wang Z, Guo F, Hu X, Wang J, Wang W, Geng C, Xu G, Wang Y, et al (2023) Enhanced cycle-capacity of micron scale silicon anode materials for lithium-ion batteries using embedded nanoparticles. *ScienceAsia* **49**, 706–709.
6. Selvarajan V, Obuobi S, Ee PLR (2020) Silica nanoparticles a versatile tool for the treatment of bacterial infections. *Front Chem* **8**, 602.
7. Dong Q, Dong A, Morigen (2015) Evaluation of novel antibacterial N-halamine nanoparticles prodrugs towards susceptibility of *Escherichia coli* induced by DksA protein. *Molecules* **20**, 7292–7308.
8. Li B, Liao Y, Su X, Chen S, Wang X, Shen B, Song H, Yue P (2023) Powering mesoporous silica nanoparticles into bioactive nanoplatforms for antibacterial therapies: strategies and challenges. *J Nanobiotechnology* **21**, 325.
9. Wang K, Wang Y, Wang C, Jia X, Li J, Xiao R, Wang S (2018) Facile synthesis of high-performance $SiO_2$@Au core–shell nanoparticles with high SERS activity. *RSC Adv* **8**, 30825–30831.
10. Stöber W, Fink A, Bohn E (1968) Controlled growth of monodisperse silica spheres in the micron size range. *J Colloid Interface Sci* **26**, 62–69.
11. Bogush G, Tracy M, Zukoski Iv C (1988) Preparation of monodisperse silica particles: control of size and mass fraction. *J Non-Cryst Solids* **104**, 95–106.
12. Matsoukas T, Gulari E (1988) Dynamics of growth of silica particles from ammonia-catalyzed hydrolysis of tetra-ethyl-orthosilicate. *J Colloid Interface Sci* **124**, 252–261.

13. da Silva AdS, Dos Santos JHZ (2023) Stöber method and its nuances over the years. *Adv Colloid Interface Sci* **314**, 102888.

14. Wang X-D, Shen Z-X, Sang T, Cheng X-B, Li M-F, Chen L-Y, Wang Z-S (2010) Preparation of spherical silica particles by Stöber process with high concentration of tetra-ethyl-orthosilicate. *J Colloid Interface Sci* **341**, 23–29.

15. Sivolapov P, Myronyuk O, Baklan D (2022) Synthesis of Stober silica nanoparticles in solvent environments with different Hansen solubility parameters. *Inorg Chem Commun* **143**, 109769.

16. Tan C, Bowen B, Epstein N (1987) Production of monodisperse colloidal silica spheres: Effect of temperature. *J Colloid Interface Sci* **118**, 290–293.

17. Giesche H (1994) Synthesis of monodispersed silica powders II. Controlled growth reaction and continuous production process. *J Eur Ceram Soc* **14**, 205–214.

18. Dong H, Han Y, Teng S, Hu Y, Guo Z, Wang D, Yang W (2021) Tetrabutylammonium bromide assisted preparation of monodispersed submicrometer silica particles. *Colloids Surf A: Physicochem Eng Asp* **614**, 126171.

19. Luo X, Dong J, Zhang L, Du J, Wang H, Gao W (2017) Preparation of silica micro spheres via a semibatch sol-gel method. *J Sol-Gel Sci Technol* **81**, 669–677.

20. Han Y, Lu Z, Teng Z, Liang J, Guo Z, Wang D, Han M-Y, Yang W (2017) Unraveling the growth mechanism of silica particles in the Stober method: *in situ* seeded growth model. *Langmuir* **33**, 5879–5890.

21. Nakabayashi H, Yamada A, Noba M, Kobayashi Y, Konno M, Nagao D (2010) Electrolyte-added one-pot synthesis for producing monodisperse, micrometer-sized silica particles up to 7 μm. *Langmuir* **26**, 7512–7515.

22. Saha A, Narula K, Mishra P, Biswas G, Bhakta S (2023) A facile cost-effective electrolyte-assisted approach and comparative study towards the Greener synthesis of silica nanoparticles. *Nanoscale Adv* **5**, 1386–1396.

23. Mazzoli A, Favoni O (2012) Particle size, size distribution and morphological evaluation of airborne dust particles of diverse woods by Scanning Electron Microscopy and image processing program. *Powder Technol* **225**, 65–71.

24. Issa AA, Luyt AS (2019) Kinetics of alkoxysilanes and organoalkoxysilanes polymerization: A review. *Polymers* **11**, 537.

25. Fernandes RS, Raimundo Jr IM, Pimentel MF (2019) Revising the synthesis of Stöber silica nanoparticles: A multivariate assessment study on the effects of reaction parameters on the particle size. *Colloids Surf A: Physicochem Eng Asp* **577**, 1–7.

26. Chang SM, Lee M, Kim W-S (2005) Preparation of large monodispersed spherical silica particles using seed particle growth. *J Colloid Interface Sci* **286**, 536–542.

27. Lee K, Look J-L, Harris MT, McCormick AV (1997) Assessing extreme models of the Stöber synthesis using transients under a range of initial composition. *J Colloid Interface Sci* **194**, 78–88.

28. Qi D, Lin C, Zhao H, Liu H, Lü T (2017) Size regulation and prediction of the $SiO_2$ nanoparticles prepared via Stöber process. *J Dispers Sci Technol* **38**, 70–74.

29. van Blaaderen A, Kentgens A (1992) Particle morphology and chemical microstructure of colloidal silica spheres made from alkoxysilanes. *J Non-Cryst Solids* **149**, 161–178.

30. Zeng D, Zhang H, Wang B, Sang K, Yang J (2015) Effect of ammonia concentration on silica spheres morphology and solution hydroxyl concentration in Stober process. *J Nanosci Nanotechnol* **15**, 7407–7411.

31. Harris MT, Brunson RR, Byers CH (1990) The base-catalyzed hydrolysis and condensation reactions of dilute and concentrated TEOS solutions. *J Non-Cryst Solids* **121**, 397–403.

32. Rao KS, El-Hami K, Kodaki T, Matsushige K, Makino K (2005) A novel method for synthesis of silica nanoparticles. *J Colloid Interface Sci* **289**, 125–131.

33. van Helden A, Jansen J, Vrij A (1981) Preparation and characterization of spherical monodisperse silica dispersions in nonaqueous solvents. *J Colloid Interface Sci* **81**, 354–368.

34. Giesche H (1994) Synthesis of monodispersed silica powders I. Particle properties and reaction kinetics. *J Eur Ceram Soc* **14**, 189–204.

35. Nagao D, Kon Y, Satoh T, Konno M (2000) Electrostatic interactions in formation of particles from tetraethyl orthosilicate. *J Chem Eng Jpn* **33**, 468–473.

36. Meier M, Ungerer J, Klinge M, Nirschl H (2018) Synthesis of nanometric silica particles via a modified Stöber synthesis route. *Colloids Surf A: Physicochem Eng Asp* **538**, 559–564.

37. Park SK, Do Kim K, Kim HT (2002) Preparation of silica nanoparticles: determination of the optimal synthesis conditions for small and uniform particles. *Colloids Surf A: Physicochem Eng Asp* **197**, 7–17.